



Generation of sub-10-fs deep and extreme ultraviolet pulses for time-resolved photoemission spectroscopy

SHUTARO KARASHIMA, CHIH-JEN CHEN, AND TOSHINORI SUZUKI*

Department of Chemistry, Graduate School of Science, Kyoto University, Kitashirakawa-Oiwakecho, Sakyo-Ku, Kyoto 606-8502, Japan
*suzuki@kuchem.kyoto-u.ac.jp

Received 25 April 2024; revised 29 May 2024; accepted 29 May 2024; posted 30 May 2024; published 27 June 2024

We present a light source capable of generating sub-10-fs deep UV (DUV) and extreme UV (EUV) pulses for use in time-resolved photoemission spectroscopy. The fundamental output of a Ti:sapphire laser was compressed using the multi-plate method and mixed with the uncompressed second harmonic in a filamentation four-wave mixing process to generate sub-10-fs DUV pulses. Sub-10-fs EUV pulses were generated via high-order harmonic generation driven by the second harmonic pulses that were compressed using Ar gas and chirped mirrors. The minimum cross correlation time between 267 and 57 nm (corresponding to 21.7 eV) was measured to be 10.6 ± 0.4 fs. © 2024 Optica Publishing Group. All rights, including for text and data mining (TDM), Artificial Intelligence (AI) training, and similar technologies, are reserved.

<https://doi.org/10.1364/OL.528323>

Time-resolved photoemission spectroscopy (TRPES) is used for observing the electronic and nuclear dynamics in atoms, molecules, and condensed matter [1–3]. TRPES requires a high probe photon energy for several reasons. First of all, soft x ray (SX) radiation is indispensable for observing the inner-shell electrons tightly bound to the nuclei. Secondly, in valence photoionization experiments, a high probe photon energy is useful for observing electronic relaxation to the ground state or the formation of ground-state products [4–8]. Last but not least, photoelectrons generated in condensed matter are inelastically scattered in the material [9–11], which is mitigated by observing electrons at high kinetic energies because of the lower scattering cross section [12,13].

High-order harmonic generation (HHG) [14,15] allows the development of table-top light sources for the extreme ultraviolet (EUV) and SX regions [16–18]. A turnkey Ti:sapphire regenerative amplifier can produce stable 800-nm pulses with a time duration of ~ 35 fs and an energy of > 2 mJ, which are sufficient for constructing a deep UV (DUV)-EUV pump-probe system with a sub-50-fs temporal resolution [8]. However, numerous applications necessitate a higher time resolution to clearly observe electronic and nuclear dynamics, prompting a desire for superior instrumental performance with minimal technical complexity. The multi-plate method [19–25] allows efficient self-phase modulation by propagating an optical pulse through a series of silica plates, enabling pulse compression to < 15 fs.

Because the time duration of the pulses produced by HHG is generally shorter than that of the input pulses, this technique enables the generation of sub-10-fs EUV pulses.

To perform TRPES, individual single-order harmonics must be isolated from the multiple-order radiation produced by HHG. Poletto *et al.* reported a time-delay-compensated monochromator (TDCM) that employs two gratings in a tandem configuration; in this system, pulse broadening induced by the first grating is compensated for by the second grating [26,27]. It has been demonstrated that a TDCM can isolate a single harmonic while maintaining a pulse duration of ~ 10 fs. As will be elaborated upon later, a TDCM yields a slightly longer pulse duration than a metallic filter, but it provides superior transmission efficiency.

To achieve a high temporal resolution in TRPES, generation of ultrashort DUV pulses is crucial. Galli *et al.* demonstrated an ultimate pulse duration of < 2 fs at ~ 260 nm through the upconversion of near-infrared pulses in a special glass cell filled with a noble gas [28]. Alternatively, filamentation four-wave mixing (FFWM) is capable of producing < 10 -fs pulses using a simple gas cell [29–34]. In the present study, we have developed a light source to generate sub-10-fs DUV and EUV pulses using FFWM and HHG, respectively, for application to TRPES.

Figure 1 shows the optical layout. The fundamental (ω) beam, generated by a Ti:sapphire regenerative amplifier (5 kHz, 35 fs, 2 mJ, 800 nm) was divided into three separate beams with pulse energies of 0.4, 0.9, and 0.7 mJ. The 0.4 mJ beam was loosely focused by a pair of concave and convex mirrors ($r = -2000$ and $+1000$ mm, respectively) separated by 670 mm. These mirrors produced a focal spot with a diameter of ~ 0.4 mm, resulting in a photon density of $< 10^{13}$ W/cm². At this density, the instability due to nonlinear optical effects in air was negligible. The focal point was positioned in front of a multi-plate system consisting of 8 synthetic fused silica plates (0.2-mm thickness) spaced ~ 10 cm apart. Figure 2(a) shows the measured spectrum of ω after passing through different numbers of plates mounted at the Brewster's angle. The pulse energy after passing through 8 plates was 0.38 mJ. The spectrally broadened ω beam was collimated using a spherical mirror ($r = -4000$ mm) to a diameter of ~ 10 mm and reflected 16 times by chirped mirrors (total -433 fs² at 800 nm) for compression. The 0.9 mJ beam was down-collimated using a pair of concave and convex mirrors ($r = -750$ and $+300$ mm, respectively) and introduced into a 0.2-mm-thick BBO crystal for second harmonic generation (SHG).

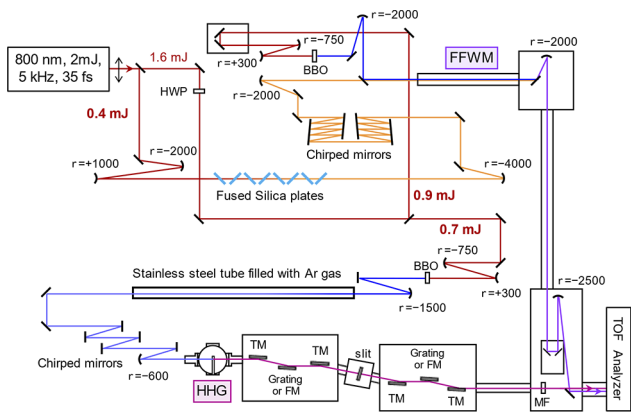


Fig. 1. Schematic diagram of the optical layout. Negative and positive values indicate the radius of concave and convex mirrors, respectively. (HWP, half wave plate; BBO, β -barium borate; TM, gold toroidal mirror; FM, gold flat mirror; MF, metallic filter.)

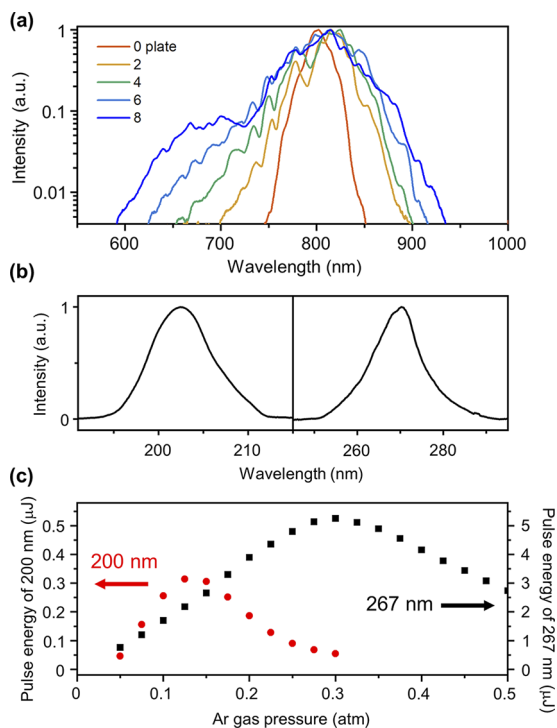


Fig. 2. (a) Spectra of 800-nm pulses broadened by self-phase modulation with multiple synthetic fused silica glass plates. The intensity is shown on a logarithmic scale. (b) Spectra of 267- and 200-nm pulses obtained by FFWM. (c) Dependence of measured pulse energies at 267 and 200 nm on Ar gas pressure.

The compressed ω pulses (0.3 mJ) and uncompressed 2ω pulses (0.24 mJ) were gently focused into an Ar gas cell with spherical mirrors ($r = -2000$ mm) through a synthetic fused silica window (0.5 mm thickness). Spatiotemporal overlap of the ω and 2ω beams induces filamentation propagation through the gas, and a cascaded four-wave mixing process generates DUV pulses. Figures 2(b) and 2(c) show the spectra of the 3ω and 4ω pulses and the variation of their intensity with Ar pressure, respectively. The time duration of the broadband 800-nm pulses was measured to be 9–10 fs with Wizzler USP-4 (FASTLITE) after

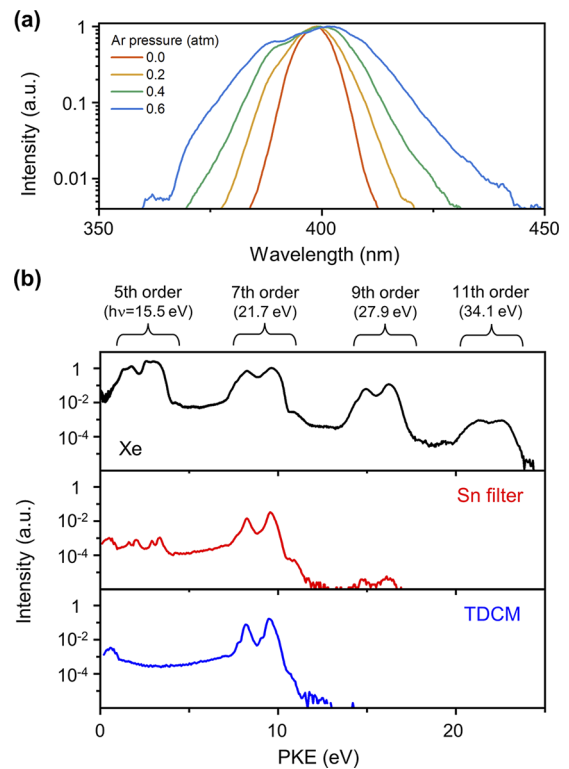


Fig. 3. (a) Spectra of 400-nm pulses broadened by self-phase modulation in Ar gas. The vertical axis is on a logarithmic scale. (b) Photoelectron spectra of Xe ionized by EUV pulses. The panels show spectra obtained using non-monochromatized EUV pulses (black) and EUV pulses monochromatized using a Sn filter (red) and a TDCM (blue). The intensity is plotted on a logarithmic scale. The bands shown in black in the upper panel are slightly broadened due to a space charge effect.

the chirp compensation. However, we found that the 800-nm pulses must have a negative chirp to generate 3ω pulses with the shortest pulse duration. The spectra of the 3ω and 4ω pulses correspond to a Fourier transform limit of 7–8 fs. The conversion efficiency from 3ω to 4ω achieved by cascaded FFWM is higher than that obtained using 25-fs driving laser pulses [34].

We utilized the 400-nm pulses for driving HHG because the harmonics generated by the 400-nm pulses are widely spaced in the wavelength and more easily monochromatized. The 0.7-mJ ω beam was down-collimated with a pair of concave and convex mirrors ($r = -750$ and $+300$ mm, respectively) and directed into a 0.2-mm-thick BBO crystal for SHG. The 2ω pulses (0.2 mJ) thus generated were focused into an Ar gas cell (0.6 atm) with a spherical mirror ($r = -1500$ mm) through a synthetic fused silica window (0.5-mm thickness). The pulse energy after passing through the gas cell was 0.18 mJ. The spectra of the transmitted 2ω pulses are shown in Fig. 3(a). The time duration of the compressed 2ω pulses was estimated to be 15–20 fs using self-diffraction frequency-resolved optical gating. These pulses underwent dispersion compensation through 5 reflections by the chipped mirrors (total -250 fs²) and were focused using a spherical mirror ($r = -600$ mm) into a HHG gas cell. The 2ω pulse energy in front of the HHG vacuum chamber was 0.14 mJ. The gas cell had a copper tube (3-mm inner diameter) filled with Ar or Kr gas at ~ 5 Torr. The vacuum chamber pressure was kept at $\sim 10^{-6}$ Torr during the operation. The high harmonics

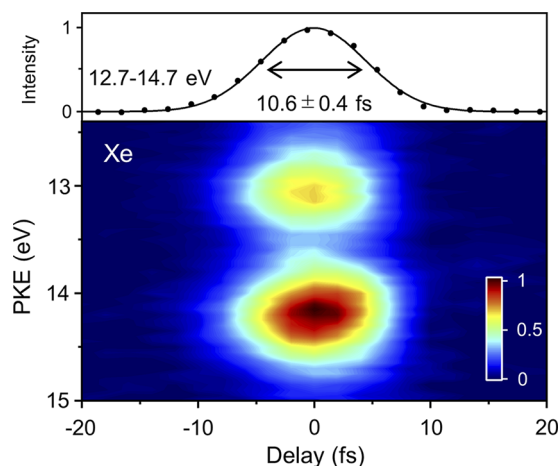


Fig. 4. Non-resonant photoionization signal for Xe using 267- and 57-nm pulses with a Sn filter. The intensity–time profile integrated over the 12.7–14.7 eV region is shown in the top panel.

were then introduced into a TDCM with 30 grooves/mm. The bandwidth of the 7th order harmonic from 2ω (Table 1, 57 nm; $h\nu = 21.7$ eV) was estimated to be ~ 0.4 eV based on measurements using the photoionization of Xe. Initially, we tested the multi-plate compression method for the 400-nm driving pulses for HHG; however, we encountered an instability and a gradually decreasing transmission efficiency due to degradation of the glass plates, which we were unable to resolve. Thus, we used the Ar gas cell. The photoelectron kinetic energy (PKE) was measured using a magnetic bottle time-of-flight electron energy analyzer [35].

Figure 3(b) compares the photoelectron spectra of Xe ionized by non-monochromatized and monochromatized EUV pulses. The 0.15- μm -thick Sn filter isolates the 57-nm pulses; however, it provides incomplete rejection of other harmonics and a relatively low transmission efficiency. The TDCM achieves complete separation of the desired harmonic, albeit with slightly greater dispersion (i.e. a longer pulse duration) compared to the filter. The pulse energy of a single harmonic was attenuated by 65 and 13 times with the Sn filter and TDCM, respectively. Using the non-resonant photoionization signal for Xe, the cross correlation time between DUV pulses produced by FFWM and EUV pulses produced by HHG was measured to be 10.6 ± 0.4 fs with the Sn filter and 13.3 ± 0.9 fs with the TDCM (Fig. 4). The two bands in Fig. 4 correspond to the doublet 2P_J ($J = 1/2$ and $3/2$) for Xe^+ .

Here we demonstrate TRPES using EUV pulses isolated with the Sn filter. The organic molecule 1,3-cyclohexadiene undergoes a ring-opening reaction to form 1,3,5-hexatriene [8,36,37]. Figure 5(a) shows TRPE spectra that we previously measured with a 48-fs time resolution and a ~ 0.1 -eV energy resolution [8]. The electron binding energy (eBE) is the difference between the probe photon energy and the observed PKE. The experimental data appears fuzzy for these fine time and energy scales. In contrast, Fig. 5(b) displays the results obtained with a time resolution of 11 fs in the present study. The results show a significant reduction in fuzziness along the time axis, making the temporal behavior of the three bands easily discernible. Bands A–C correspond to the photoionization from the excited state S_1 to the three lowest cationic states D_0 , D_1 , and D_2 , respectively. Figure 5(c) shows the TRPE spectra theoretically simulated using

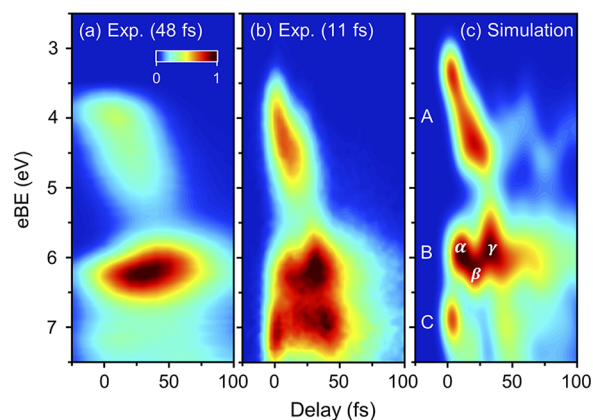


Fig. 5. Two-dimensional maps of photoelectron spectra measured for 1,3-cyclohexadiene using 267- and 57-nm pulses with a cross correlation time of (a) 48 fs [8] and (b) 11 fs in this study. (c) Theoretically calculated map [8]. The theoretical results were convoluted with a Gaussian function with temporal and energy widths of 11 fs and 0.4 eV (FWHM), respectively.

Table 1. Laser Pulse Parameters

	λ/nm	Time Duration /fs	Energy/ μJ
Laser	800	35	2000
Input	FFWM	800	9–10
	HHG	400	35 <
	FFWM	267	$< 8^a$
Output	FFWM	200	$< 8^a$
	HHG	80, 57, 44, 36	$\sim 7^a$

^aFourier transform limit estimated from the spectral bandwidth.

trajectory surface hopping calculations with the highly accurate XMS-CASPT2 (extended complete active space second-order perturbation theory) electronic structure method [8,36]. Band B is slightly shifted to a higher eBE value at 20 fs (β) and returns to a lower value at 35 fs (γ). The oscillatory feature $\alpha \rightarrow \beta \rightarrow \gamma$ originates from the conical intersection between the cationic state potentials upon lengthening of the dissociating C–C bond. The clear agreement between Figs. 5(b) and 5(c) highlights the utility of the new light source.

In summary, we developed a light source that generates sub-10-fs DUV and EUV pulses for TRPES (Table 1). A thin Sn filter yields a minimum cross correlation time of 10.6 fs, while a TDCM achieves complete monochromatization and relatively high transmittance for a single-order harmonic and a cross correlation time of 13.3 fs. The light source allowed us to extract more detailed features related to the photodynamics of 1,3-cyclohexadiene.

Disclosures. The authors declare no conflicts of interest.

Data availability. The data underlying the results presented in this paper are not publicly available at this time but may be obtained from the authors upon reasonable request.

REFERENCES

- A. Stolow, A. E. Bragg, and D. M. Neumark, *Chem. Rev.* **104**, 1719 (2004).
- I. V. Hertel and W. Radloff, *Rep. Prog. Phys.* **69**, 1897 (2006).

3. T. Suzuki, *Annu. Rev. Phys. Chem.* **57**, 555 (2006).
4. A. D. Smith, E. M. Warne, D. Bellshaw, *et al.*, *Phys. Rev. Lett.* **120**, 183003 (2018).
5. M. Puppini, Y. Deng, C. W. Nicholson, *et al.*, *Rev. Sci. Instrum.* **90**, 023104 (2019).
6. J. H. Buss, H. Wang, Y. Xu, *et al.*, *Rev. Sci. Instrum.* **90**, 023105 (2019).
7. Y. Liu, S. L. Horton, J. Yang, *et al.*, *Phys. Rev. X* **10**, 021016 (2020).
8. S. Karashima, A. Humeniuk, R. Uenishi, *et al.*, *J. Am. Chem. Soc.* **143**, 8034 (2021).
9. Y.-I. Suzuki, K. Nishizawa, N. Kurahashi, *et al.*, *Phys. Rev. E* **90**, 010302 (2014).
10. T. Suzuki, *J. Chem. Phys.* **151**, 090901 (2019).
11. A. Jablonski and C. J. Powell, *J. Phys. Chem. Ref. Data* **49**, 033102 (2020).
12. C. F. Perry, I. Jordan, P. Zhang, *et al.*, *J. Phys. Chem. Lett.* **12**, 2990 (2021).
13. Y. Yamamoto and T. Suzuki, *J. Phys. Chem. A* **127**, 2440 (2023).
14. M. Ferray, A. L'Huillier, X. F. Li, *et al.*, *J. Phys. B: At. Mol. Opt. Phys.* **21**, L31 (1988).
15. P. B. Corkum, *Phys. Rev. Lett.* **71**, 1994 (1993).
16. Z. Chang, A. Rundquist, H. Wang, *et al.*, *Phys. Rev. Lett.* **79**, 2967 (1997).
17. C. Spielmann, N. H. Burnett, S. Sartania, *et al.*, *Science* **278**, 661 (1997).
18. M. Hentschel, R. Kienberger, C. Spielmann, *et al.*, *Nature* **414**, 509 (2001).
19. C.-H. Lu, Y.-J. Tsou, H.-Y. Chen, *et al.*, *Optica* **1**, 400 (2014).
20. Y.-C. Cheng, C.-H. Lu, Y.-Y. Lin, *et al.*, *Opt. Express* **24**, 7224 (2016).
21. P. He, Y. Liu, K. Zhao, *et al.*, *Opt. Lett.* **42**, 474 (2017).
22. C.-H. Lu, W.-H. Wu, S.-H. Kuo, *et al.*, *Opt. Express* **27**, 15638 (2019).
23. M. Seo, K. Tsendsuren, S. Mitra, *et al.*, *Opt. Lett.* **45**, 367 (2020).
24. B. Zhu, Z. Fu, Y. Chen, *et al.*, *Opt. Express* **30**, 2918 (2022).
25. J. I. Kim, Y. G. Kim, J. M. Yang, *et al.*, *Opt. Express* **30**, 8734 (2022).
26. M. Eckstein, C.-H. Yang, M. Kubin, *et al.*, *J. Phys. Chem. Lett.* **6**, 419 (2015).
27. L. Poletto and F. Frassetto, *Appl. Sci.* **8**, 5 (2018).
28. M. Galli, V. Wanie, D. P. Lopes, *et al.*, *Opt. Lett.* **44**, 1308 (2019).
29. T. Fuji, T. Horio, and T. Suzuki, *Opt. Lett.* **32**, 2481 (2007).
30. T. Fuji, T. Suzuki, E. E. Serebryannikov, *et al.*, *Phys. Rev. A* **80**, 063822 (2009).
31. M. Beutler, M. Ghotbi, F. Noack, *et al.*, *Opt. Lett.* **35**, 1491 (2010).
32. M. Ghotbi, M. Beutler, and F. Noack, *Opt. Lett.* **35**, 3492 (2010).
33. M. Ghotbi, P. Trabs, M. Beutler, *et al.*, *Opt. Lett.* **38**, 486 (2013).
34. T. Horio, R. Spesytysev, and T. Suzuki, *Opt. Express* **21**, 22423 (2013).
35. N. Kurahashi, S. Thürmer, S. Y. Liu, *et al.*, *Struct. Dyn* **8**, 034303 (2021).
36. I. Polyak, L. Hutton, R. Crespo-Otero, *et al.*, *J. Chem. Theory Comput.* **15**, 3929 (2019).
37. O. Travnikova, T. Piteša, A. Ponzi, *et al.*, *J. Am. Chem. Soc.* **144**, 21878 (2022).